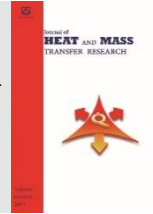




Semnan University



## Research Article

# Thermo-Hydraulic Performance of Tube Type Heat Exchanger with Semi-Circular Cut Twisted Tape Insert: A Numerical Exploration

Manoj Kumar Diwaker\*, , Arvind Kumar 

Department of Mechanical Engineering MANIT Bhopal, 462003, India.

## PAPER INFO

### Paper history:

Received: 2023-04-24

Revised: 2023-10-03

Accepted: 2023-10-04

### Keywords:

Tube type heat exchanger;  
Convective heat transfer;  
Heat transfer coefficient;  
Friction Factor;  
Nusselt Number.

## ABSTRACT

The present study aimed to investigate the effects of the semi-circular cut twisted tape insert in tube type heat exchangers. The study selected twist ratios of 4.5, 5.5, and 6.5mm, and cut diameters of 5mm, 8mm, and 11mm. The Reynolds number ranged from 4000-16000. The study quantitatively demonstrated the impacts of cut diameter and twist ratio in terms of Nusselt number, friction factor, and thermal performance factor. The aforementioned output parameters were employed as metrics to assess the efficacy of the twisted tape insert. The obtained results reveal that smaller twist generates extra swirl which intensifies heat transfer. Also, as the diameter of the cut increases Nusselt number increases. In a quantitative analysis, it was observed that when  $Re=4000$ , the plain twisted tapes with  $y=4.5, 5.5,$  and  $6.5$  exhibited maximum thermal performance factors of 1.36, 1.32, and 1.21, respectively. On the other hand, for the modified twisted tapes (having a cut diameter of 11mm), the values were higher, measuring 1.84, 1.77, and 1.68 for the same respective 'y' values.

DOI: [10.22075/jhmtr.2023.30445.1438](https://doi.org/10.22075/jhmtr.2023.30445.1438)

© 2023 Published by Semnan University Press. All rights reserved.

## 1. Introduction

The fascination with energy demand and escalating heat transfer requirements has captivated the attention of researchers in this realm. Over the recent decades, there has been a notable surge in the adoption of single-phase heat exchange apparatus. This surge can be attributed to the burgeoning need for heightened heat transfer efficiency across various industries. Consequently, a multitude of technologies have surfaced, aiming to enhance heat transfer rates. These innovative techniques are devised to augment heat transfer efficiency by incorporating turbulence-inducing mechanisms such as inserts, artificially roughened tubes, ribs, rib-groove configurations, blocks, fins, barriers, turbulators, and swirling devices like twisted tape inserts, winglets, wire rings, coiled wires, and more. This progression in heat transfer technology has profoundly shaped the evolution of heat

exchangers, enabling them to adeptly shuttle heat between two fluids. For example, the integration of inserts in heat exchangers has been proven to elevate heat transfer rates by instigating turbulence conducive to efficient heat exchange. Conversely, artificially roughened tubes are engineered with inward projections to provoke turbulence, thus amplifying heat transfer rates. In air conditioning systems, rib-groove heat exchangers have emerged as effective tools for intensifying heat transfer. The incorporation of grooves in these exchangers escalates fluid flow turbulence, leading to heightened heat transfer rates. Moreover, the introduction of fins escalates the heat transfer surface area between fluids, facilitating swifter and more proficient heat exchange. Passive techniques like artificial roughness and swirl flow devices substantively elevate heat transfer rates and pressure drops compared to smooth tubes. Although the inclusion of

\*Corresponding Author: Manoj Kumar Diwaker.

Email: [mdiwakermanit@gmail.com](mailto:mdiwakermanit@gmail.com)

inserts within tubular heat exchangers notably bolsters the heat transfer coefficient, it does come at the expense of increased friction factor levels. Numerous researchers have amassed insights into diverse heat transfer augmentation methods encompassing active, passive, and combined approaches. Interestingly, passive techniques seem to garner more attention.

For Instance, Wijayanta et al. [1] conducted an experimental investigation on a double pipe heat exchanger that incorporates double-sided delta winglet tapes. The central objective of this study was to determine how well three distinct delta winglets, each with a different wing width ratio of 0.31, 0.47, or 0.63, performed in terms of their effectiveness. To investigate the effectiveness of different delta winglets, the authors conducted experiments with the aforementioned three different wing width ratios. The experiment involved incorporating delta winglets, which are small triangular protrusions, into the design of the heat exchanger. The purpose of incorporating the delta winglets was to investigate their effect on the heat transfer performance of the heat exchanger. The investigation into the impact of baffle orientation on the performance of shell-and-tube heat exchangers has been carried out by a group of researchers led by Abbasian Arani et al. [2]. The study conducted by Wijayanta et al. contributes to the development of more efficient heat exchangers in various industries, such as chemical processing, power generation, and refrigeration. After a numerical investigation Wijayanta et al. [3] concluded that TPF was increased in turbulent regime with short length twisted tapes and Nu increased by 81% in DPHE. For square cut TT in the turbulent area, numerical study of DPHE by Wijayanta et al. [4] estimated the Nu. In comparison to plain tube, the maximum increase in Nu was reported 177% .

The fascination with energy demand and escalating heat transfer requirements has captivated the attention of researchers in this realm. Over the recent decades, there has been a notable surge in the adoption of single-phase heat exchange apparatus. This surge can be attributed to the burgeoning need for heightened heat transfer efficiency across various industries. Consequently, a multitude of technologies have surfaced, aiming to enhance heat transfer rates. These innovative techniques are devised to augment heat transfer efficiency by incorporating turbulence-inducing mechanisms such as inserts, artificially roughened tubes, ribs, rib-groove configurations, blocks, fins, barriers, turbulators, and swirling devices like twisted tape inserts, winglets, wire rings, coiled wires, and more. This progression in heat transfer technology has profoundly shaped the evolution of heat exchangers, enabling them to adeptly shuttle heat between two fluids. For example, the integration of inserts in heat exchangers has been proven to elevate heat transfer rates by instigating turbulence conducive to efficient heat exchange. Conversely, artificially

roughened tubes are engineered with inward projections to provoke turbulence, thus amplifying heat transfer rates. In air conditioning systems, rib-groove heat exchangers have emerged as effective tools for intensifying heat transfer. The incorporation of grooves in these exchangers escalates fluid flow turbulence, leading to heightened heat transfer rates. Moreover, the introduction of fins escalates the heat transfer surface area between fluids, facilitating swifter and more proficient heat exchange. Passive techniques like artificial roughness and swirl flow devices substantively elevate heat transfer rates and pressure drops compared to smooth tubes. Although the inclusion of inserts within tubular heat exchangers notably bolsters the heat transfer coefficient, it does come at the expense of increased friction factor levels. Numerous researchers have amassed insights into diverse heat transfer augmentation methods encompassing active, passive, and combined approaches. Interestingly, passive techniques seem to garner more attention.

Additionally, it was shown that a smaller twist ratio causes a greater thermal performance factor. With various modified twisted tapes, Murali et al. [5] used CFD tool for the investigation of the impacts of cut on insert in DPHE. They concluded that  $Fe_2O_3$ -Water nanofluid was found to improve heat transmission by 35.63% at Reynolds number 12000. In a study conducted by P.V. Prasad et al. [6], a U-tube heat exchanger with a trapezoidal cut insert was used to examine the effects of  $Al_2O_3$ -Water nanofluid. A significant improvement in the maximum heat transfer rate was reported by them, with an increase of 34.24%. The Reynolds number range examined in their study was 3000-30000. The impact of a V-cut insert on the enhancement of heat transfer operating with single-phase turbulent flow was investigated by Yaningsih et al. [7]. Their findings revealed a remarkable augmentation in both heat transfer and friction factor, reaching as high as 97% and 3.48 times that of a conventional plain tube, respectively. The peak thermal performance achieved was 1.4. In a study conducted by Singh and Kumar [8], the influence of dimple inserts in turbulent flow conditions was investigated. The researchers aimed to determine how different dimple geometries affected the performance enhancement coefficient (PEC) in turbulent flow. Their study indicates that the shape of the dimple has a significant impact on its effectiveness in improving flow performance. Overall, this research highlights the importance of understanding the impact of different geometries on the performance of flow-enhancing devices like dimple inserts. Further studies can build on these findings to improve the design and implementation of these devices for various applications, such as in the aerospace and automotive industries. In an experimental study of DPHE using IoT approach conducted by Diwaker and Kumar [9] reported the maximum TPF 1.531 in case of combined circular and

semi-circular cut. In a separate experimental study of DPHE using IoT approach conducted by Diwaker and Kumar [10], the maximum TPF of 1.592 is reported. Triangular and semi-circular cut in a plain twisted taped were taken for the investigation. A study conducted by Rezaei and Baniamerian [11] delved into the assessment of hydro-thermal performance of nanofluids flow in a DPHE. The investigation specifically considered the impact of the inner pipe's cross-sectional shape, which could either be circular or cam-shaped. Meanwhile, the thermal effects of introducing pitch-length louvered strips into a concentric pipe heat exchanger were explored by Yaningsih and Wijayanta [12]. Across all scenarios, in steady state, with Reynolds numbers spanning from 5300 to 17,500. Notably, the findings indicated that the incorporation of louvered strip inserts led to notably heightened heat transfer rates in comparison to the use of plain tubes. Akbarzadeh et al. [13] analyzed the effect of porous inserts on DPHE. They suggested that it intensifies the heat transfer if it is kept near the inner wall. Mohammad Soltani et al. [14] studied DPHE with dimple TT under turbulent regime and achieved a maximum TPF 1.24. In a study conducted by Dandoutiya and Kumar [15], triangular cut TT in DPHE through numerical simulations has been investigated. The findings of their investigation revealed significant improvements in performance characteristics. They achieved a maximum TPF of 1.21. In a related study, Wijayanta et al. [16] performed CFD analysis on a tube boosted with backward louvered inserts. The computational findings displayed that the Nu numbers were amplified to 1.81, 1.75, and 1.72 times in the studied cases. Similarly, the maximum factor of friction increases of 7.59 times compared to the plain tube. Another investigation by Wijayanta et al. [17] delved into internal flow enhancements using square-cut twisted tape inserts in an enhanced tube. They achieved a peak thermal performance of 1.18. Arasteh et al. [18] and his team conducted a thorough investigation into the impact of metal foam inserts on the performance of a twin pipe heat exchanger. The researchers reported the heat transfer rates increased by an impressive 69%. Additionally, the researchers also discovered that the performance evaluation criterion (PEC) achieved a maximum value of 1.36, indicating that the heat exchanger operated at a highly efficient level. The greatest TPF value in the experiment performed by Azmi et al. [19] found to be between 1.141 and 1.801. Eiamsa-Ard et al. [20] concluded that with the increase of concentration of nanoparticles in the base fluid the Nusselt number improves. Wongcharee et al. used the corrugated type tube in turbulent regime. The concentrations of the nanofluids have been opted 0.3%, 0.5%, and 0.7%. and twisted tape had greater values than the individual approaches. Esmaeilzadeh et al. [21] examined how the inclusion of twisted tape inserts affects the thermo-hydraulic performance of circular

tube exchangers. Meanwhile, in their research, they found that thicker inserts produce a more favourable effect, with thicknesses ranging from 0.2mm to 0.5mm. Two different types of twisted tapes in the solar water heater have been examined by Saravanan and Jaisankar [22]. They performed the investigation with twist ratio 3.0. They concluded that the specified tapes are more effective due to bidirectional swirl generation inside the tube. In their study, Han et al. [23] utilized response surface methodology to numerically investigate a single corrugated tube. Their results reveals that the optimum values of the ratio of friction factor is  $f/f_0=1.22$  while thermal performance factor  $\eta=1.42$  for  $Nu/Nu_0=1.2$ . García et al. [24] performed their experiments with three types artificially roughened tube that are corrugated tube, wire coils and dimpled tube. In a separate study, Moya-Rico et al. [25] focused on the use of regularly spaced twisted tape inserts in a heat exchanger. The researchers found that shorter spacers resulted in higher rates of heat transfer. These findings suggest that optimizing the design of heat exchangers through the use of strategically placed inserts can yield significant improvements in their overall performance. By leveraging the latest research in the field, engineers and scientists can develop more efficient and effective heat exchangers that meet the growing demand for energy-efficient solutions. Muhammad Mostafa Kamal Bhuiya et al. [26] used perforated triple twisted tapes and reported a 4.2 times increase in the highest heat transfer and a 4.5 times increase in the friction factor. Nakhchi and Esfahani [27] used perforated elliptic turbulators in DPHE and achieved a maximum thermal performance factor value of 1.849, with a 39.4% increase in heat transfer and a 14.0% increase in the ff. M.R. According to Salem et al. [28], the DPHE was investigated with the use of helical tape inserts. Furthermore, Patel et al. [29] used ACCT in their experiment. The enhanced heat transfer coefficient can be attributed to the increased flow turbulence generated by the swirl tape, while the increased pressure drop may be due to the additional frictional resistance offered by the tape inserts. Yadav et al. [30] have employed short-length twisted tapes in the context of concentric tube U-bend heat exchangers. Short-length twisted tapes are particularly advantageous because they can be accommodated in tight spaces and are less prone to fouling compared to longer tapes. By leveraging this technology, Yadav et al. have demonstrated the potential for improved performance and energy efficiency in U-bend heat exchangers. They reported PEC 1.3-1.5 times enhanced relative to smooth tube. Muñoz-Esparza and Sanmiguel-Rojas [31] used helical wire coils placed within a circular pipe for the intensification of heat transfer. As turbulators, Karakaya and Durmus et al. [32] used conical-shaped springs. They discovered that when the conical angle rises, the exergy loss decreases. This is because the addition of tabulators to the flow medium results in

augmented thermohydraulic performance. Nakhchi et al. [33] investigated several heat exchanger designs for improving the waste heat recovery from diesel exhaust. In their research, Sheikholeslami et al. [34] introduced an innovative approach to enhance heat transfer efficiency in DPHE. They incorporated an agitator into the system and found significant improvements in thermohydraulic performance.

In summary, the development of various turbulence promoters and heat transfer technologies has significantly improved the efficiency of heat transfer in various industries. The use of these technologies in heat exchangers has resulted in more efficient heat transfer rates, which has contributed to the overall energy efficiency of many systems. The effect of TT and their alterations on improving heat transfer in a multitude of scenarios has been thoroughly explored in existing literature. Modified twisted tapes in plain tube with or without nanofluids [35-47] such as Dimpled TT [8], WC [48], ACCT [49], VC [50], SC [50], and CP [51], triangular and semi-circular cut [10] have been numerically and/or experimentally investigated. The performance enhancement coefficient (PEC), thermal performance factor (TPF), Nusselt number, and friction factor are the key parameters used to evaluate the performance of the DPHEs. Some of the commonly used inserts in DPHEs are dimple inserts, porous inserts, twisted tape inserts, metal foam inserts, regularly spaced twisted tape inserts, perforated triple twisted tapes, double-sided delta wing tape inserts, helical wire coil inserts, perforated elliptical turbulators, and helical tape inserts. The choice of the insert depends on the specific application and the desired performance enhancement. From the intensive literature review it has been concluded that there is no quantitative evaluation of the effect of semi-circular-cut diameter in the tube type heat exchangers.

However, despite the vast research on TT in tube heat exchangers, the impact of semi-circular cut diameter on heat transfer enhancement has remained unstudied. This gap in research presents a valuable opportunity to investigate the effects of semi-circular cut diameter on heat transfer enhancement. Therefore, a numerical study has been carried out to investigate the impact of the semi-circular cut twisted tape insert in the tube type heat exchanger. While the twist ratios were chosen at 4.5, 5.5, and 6.5mm, the cut diameters were chosen at 5mm, 8mm, and 11mm. In this study, the Reynolds number ranges from 4000- 16000. In the current study, the impacts of cut diameter and twist ratio are quantitatively demonstrated in terms of TPF.

## 2. Model and Methods

The 3-dimensional CAD model has been shown in Figure 1 which illustrates the arrangement of twisted tape in a tube. The analysis was carried out using a

cylindrical tube with a diameter of 25mm and a length of 1000mm. The tube had a thickness of 1.5mm.

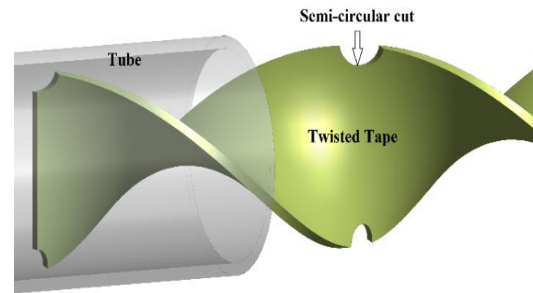


Figure 1. 3-D model of tube with semi-circular cut insert

### 2.1. Underlying Physics, Governing Equations and Boundary Conditions

The computational simulations were conducted using the Ansys Fluent 2021 R1. The FVM was employed for these simulations. The standard pressure solver was utilized, employing the second-order upwind scheme for spatial discretization. The energy and momentum equations have been solved using the numerical methods. For the coupling of pressure and velocity, the SIMPLE algorithm was adopted. In order to ensure the accuracy of the CFD model, a tetrahedron-cell mesh configuration was consistently employed across all cases. The mesh was regenerated as depicted in Figure 2. Additionally, an edge sizing method was applied in specific areas of the model. The inflation layers have been introduced near the boundaries as illustrated in Figure 2. To ensure grid independence and density, edge sizing was also implemented. A skewness value of approximately 0.21, indicating the effectiveness of the grid system. Out of the various turbulence models available, it has been revealed that the SST  $k-\omega$  turbulence model yields the most precise outcomes. Consequently, in this study, turbulent flow simulations were conducted using the SST  $k-\omega$  turbulence model. The validity of the simulations was established by comparing them to three-dimensional experimental data from previous research. The fundamental presumption was that the fluid movement stayed incompressible and followed the principles set out by Newton. Aspects like radiation and gravitational forces were not taken into account, and a no-slip boundary condition was enforced. To simulate the governing equations of turbulent flow, the algebraic equations governing mass, momentum, energy, turbulent kinetic energy ( $k$ ), and specific dissipation ( $\omega$ ) have been discretized using the second order upwind strategy in a three-dimensional computing domain. The SST  $k-\omega$  turbulence model in ANSYS CFD is a two-equation model that combines the  $k-\epsilon$  and  $k-\omega$  turbulence models to improve accuracy and robustness, especially near the walls.

These equations are a set of partial differential equations that describe the behaviour of fluid flow under certain assumptions, including the assumption that the fluid is incompressible and has a constant viscosity. The conservation of mass in a fluid system is expressed by the continuity equation.

This equation states that the net rate of mass flow into or out of a control volume is equal to the rate of change of mass within the volume. On the other hand, the conservation of momentum is expressed by the momentum equation. It relates the forces acting on the fluid to the changes in velocity. Finally, the energy equation expresses the conservation of energy, relating the changes in temperature to the heat transfer and work done on the fluid.

Expressing these equations mathematically and solving them numerically is a crucial step in understanding and predicting fluid behaviour in various engineering and scientific applications. Convergence of the solution was achieved when the residuals of the continuity, momentum, and energy equations dropped below the thresholds of  $1 \times 10^{-2}$ ,  $1 \times 10^{-4}$ , and  $1 \times 10^{-6}$ , respectively. The model equations in a general form are as follows:

Continuity Equation:

$$\nabla \cdot (\rho \vec{V}) = 0 \tag{1}$$

Momentum Equation:

$$\nabla \cdot (\rho \vec{V}\vec{V}) = -\nabla P + \mu \nabla^2 \vec{V} + \rho \vec{g} \tag{2}$$

Energy equation:

$$A_1 = \frac{\partial v}{\partial x} + \frac{\partial u}{\partial y} \tag{3}$$

$$B_1 = \frac{\partial v}{\partial x} + \frac{\partial u}{\partial y} \tag{4}$$

$$C_1 = \frac{\partial w}{\partial y} + \frac{\partial v}{\partial z} \tag{5}$$

$$D_1 = \frac{\partial u}{\partial z} + \frac{\partial w}{\partial x} \tag{6}$$

$$E = 2[A_1] + (B_1)^2 + (C_1)^2 + (D_1)^2 \tag{7}$$

$$\nabla \cdot (\rho C_p \vec{V}T) = K_{eff} \nabla^2 T + \mu E \tag{8}$$

The turbulent kinetic energy  $k$ , and  $\omega$  for the  $k$ - $\omega$  model is given by:

$$\begin{aligned} & \frac{\partial}{\partial t}(\rho k) + \frac{\partial}{\partial x_i}(\rho k u_i) \\ & = \frac{\partial}{\partial x_j} \left[ \left( \mu + \frac{\mu_t}{\sigma_k} \right) \frac{\partial k}{\partial x_j} \right] + G_k - Y_k + S_k \end{aligned} \tag{9}$$

Specific Dissipation Rate ( $\omega$ )

$$\begin{aligned} & \frac{\partial}{\partial t}(\rho \omega) + \frac{\partial}{\partial x_i}(\rho \omega u_i) \\ & = \frac{\partial}{\partial x_j} \left[ \left( \mu + \frac{\mu_t}{\sigma_\omega} \right) \frac{\partial \omega}{\partial x_j} \right] + G_\omega - Y_\omega + S_\omega \end{aligned} \tag{10}$$

Turbulent Kinetic Energy ( $k$ )

where;

$$\sigma_{\omega,1} = 2.0, \sigma_{k,1} = 1.176, \sigma_{\omega,2} = 1.168, \sigma_{k,2} = 1.0$$

There are constant temperatures of  $T_i = 300$  K and  $T_s = 313$  K on its boundary conditions.

### 2.2. Mesh Independency Test

The relative Nusselt numbers and friction factors at different number of meshes have been compared. Table 1 illustrate the relative errors in the Nusselt numbers and friction factors and Fig. 2(e) represents the variation of the Nusselt number with number of meshes at fixed  $Re=4000$ . The finer mesh gives better result but there is increase in the computational time. So the optimum mesh number of order 10,000,000 has been selected for the entire computation. Also at this mesh number the relative difference in the Nusselt number and friction factor has been found 0.01129 and 0.047 respectively instead of 0.14915 and 0.105 respectively at mesh of order 5200000. This signifies that the mesh of order 1,000,000 is relatively independent and optimum results can be obtained.

**Table 1.** The result of mesh independency test

| Number of Mesh | $Nu$ at $Re=4 \times 10^3$ | $\left  \frac{Nu^{n+1} - Nu^n}{Nu^n} \right $ | $f$ at $Re=4 \times 10^3$ | $\left  \frac{f^{n+1} - f^n}{f^n} \right $ |
|----------------|----------------------------|---|---------------------------|--|
| 1585934        | 24.61                      | -   | 0.030                     | -  |
| 3225647        | 33.12                      | 0.34579                                       | 0.038                     | 0.266                                      |
| 5234857        | 38.06                      | 0.14915                                       | 0.042                     | 0.105                                      |
| 10221455       | 38.49                      | 0.01129                                       | 0.044                     | 0.047                                      |

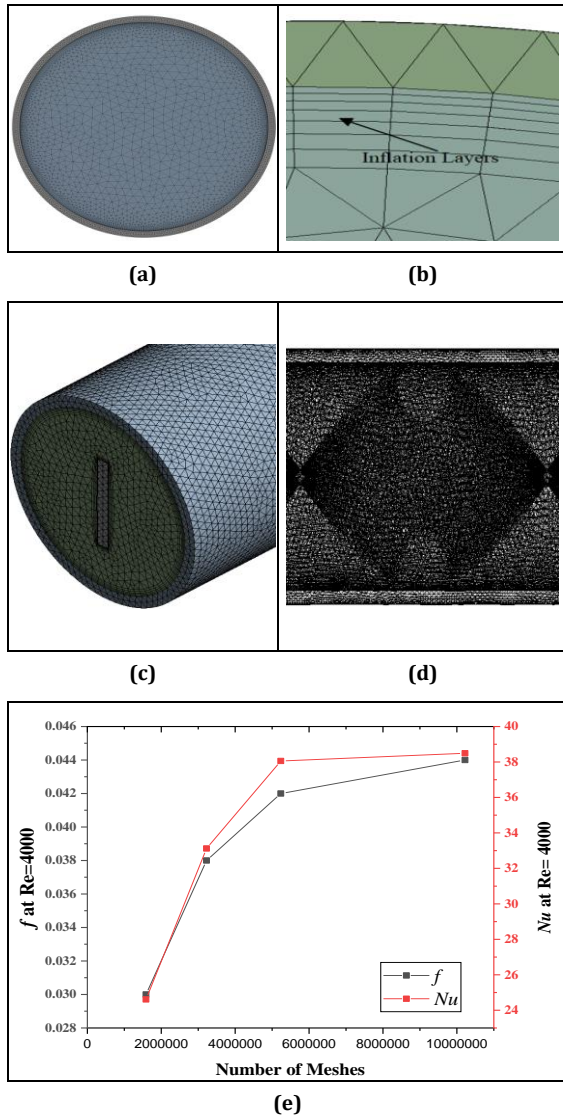


**Figure 2.** Detailed Mesh Structures (a) Cross-sectional view of plain tube mesh (b) Zoomed view of inflation layers (c) 2 Dimensional mesh of insert in tube (d) 3 Dimensional mesh of twisted tape with semi-circular cut (e) Variation of Nusselt number and Friction factor with number of meshes at Re=4000.

### 3. Data Reduction

Non-dimensional quantities like Nusselt Number, Friction Factor, and Reynolds Number may be estimated using the raw data obtained from the numerical simulation. Assuming the outer surface of the tube completely adiabatic, the following equations have been adopted for conversion of raw data into output parameters.

For Reynolds number, the following equation can be used.

$$Re = \frac{\rho V D}{\mu} \quad (11)$$

Under adiabatic conditions:

$$Q_{\text{water}} = Q_{\text{convection}} \quad (12)$$

The water's heat gain may be expressed as:

$$Q_{\text{water}} = m C_p (T_{\text{out}} - T_{\text{in}}) \quad (13)$$

$$Q_{\text{convection}} = h A_s (T_s - T_b) \quad (14)$$

$$A_s = \pi D L \quad (15)$$

$$h = \frac{m C_p (T_{\text{out}} - T_{\text{in}})}{A_s (T_s - T_b)} \quad (16)$$

The average or mean Nusselt number can be computed as:

$$Nu = \frac{h D}{k} \quad (17)$$

$$f = \frac{2 D \Delta P}{L \rho V^2} \quad (18)$$

$$T_b = \frac{T_{\text{in}} + T_{\text{out}}}{2} \quad (19)$$

## 4. Result and Discussion

### 4.1 Validation of Numerical Model

The Nusselt number and friction factor deduced from the numerical simulation have been validated through the experimental results obtained from Chaitanya Vashista et al. [40] as well as standard correlations like Dittus-Boelter correlation and Gnielinski correlation for Nusselt number and Blasius correlation and Petukhov correlation for friction factor.

Dittus-Boelter correlation:

$$Nu = 0.023 Re^{0.8} Pr^{0.4} \quad (20)$$

Gnielinski correlation

$$Nu = \frac{\frac{f}{8} (Re - 1000) Pr_f}{1 + 12.7 \sqrt{\frac{f}{8}} (Pr_f^{\frac{2}{3}} - 1)} \left[ 1 + \left( \frac{d}{l} \right)^{\frac{2}{3}} \right] c_t \quad (21)$$

where f is calculated by Petukhov correlations which is given by

$$f = [0.790 \ln(Re) - 1.64]^{-2}$$

Blasius correlation:

$$f = 0.316 Re^{-0.25} \quad (22)$$

The calculated Nu values have been verified using several correlations: the Dittus-Boelter correlation (Equation 20) with a maximum deviation of  $\pm 6.2\%$ , the Gneilnski correlations (Equation 21) with a maximum deviation of  $\pm 5.8\%$ , and the results from Chaitanya Vashistha with a maximum deviation of  $\pm 4.2\%$ . The friction factor ( $f$ ) in this study has been compared to the Blasius correlation (Equation 22) with a maximum deviation of  $\pm 6.65\%$ , the Petukhov correlation with a maximum deviation of  $\pm 7.2\%$ , and again with the Chaitanya Vashistha results with a maximum deviation of  $\pm 4.6\%$ . It's evident that the differences between the outcomes of this study and the established correlations were minimal across all analyzed scenarios. As a result, it's reasonable to conclude that the numerical approach employed in this study in stills a high level of confidence. The alignment between this study's findings and the accepted correlations was consistently close, indicating that the current calculations are significantly accurate. Therefore, we can confidently assert that the numerical model presented in this study is reliable and holds potential for predicting performance improvements in tube-type heat exchangers.

Figure 3 and Figure 4 illustrate the validation of the Nusselt number and friction factor, respectively. The comparative study of the results reveals that there is acceptable variation in the Nusselt number and friction factor.

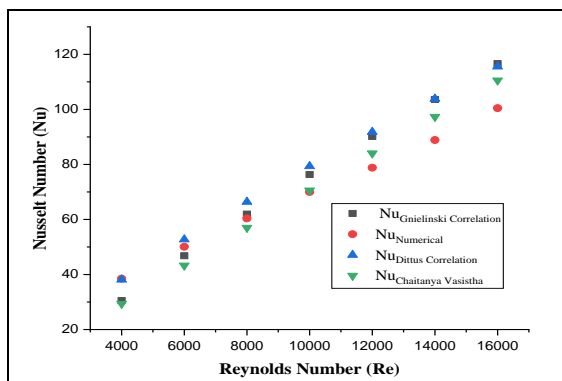


Figure 3. Validation of Nusselt Number with Experimental results and standard correlations

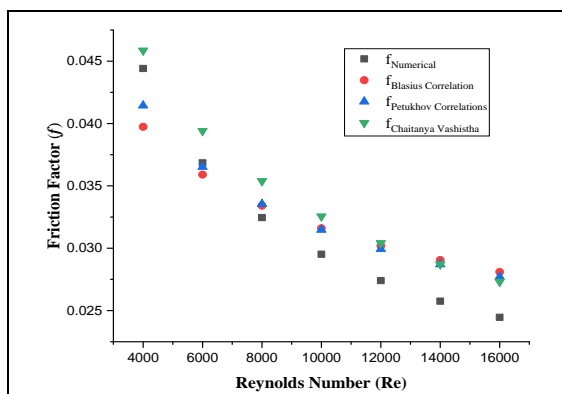


Figure 4. Validation of friction factor with Experimental results and standard correlations

#### 4.2 Heat Transfer and Friction Factor Analysis

From Figure 3 it can be visualize that Nusselt number increases as the Reynolds number increases which is due to the fact that higher mass flow rate delivers higher heat per unit time.

On the other hand Figure 4 states that friction factor decreases with the Reynolds number. The reason behind this is with increase in mass flow rate velocity of the fluid increases which in turn reduces the effect of friction.

From Figure 5 it has been shown the trend of increase of Nusselt number. A proportional increase in the Nusselt number with Reynolds number has been observed. This is due to the fact that with increase in the Reynolds number mass flow rate increases and higher mass flow rate means higher heat transport per unit time. This enhances the heat transfer rate. Twisted tapes create advance heat exchange surroundings by enhancing the turbulence of fluid which causes depletion of boundary layer. The lower twist ratio creates the higher turbulence intensity and hence higher friction factor. SCTT contributes the turbulence intensity and pressure drop. As the diameter of semi-circular cut increases from 5mm to 11mm this intensity monotonically increases. The synergy between a lower twist ratio and a larger cut diameter fosters favourable conditions for improving heat transfer characteristics holistically. Moreover, the size of the semi-circular cut significantly impacts the Nusselt number, exhibiting a direct correlation between increasing cut diameter and Nusselt number. The maximum value of Nusselt number has been found 196.38 which have been obtained at a combination of twist ratio 4.5 and the cut diameter 11 mm.

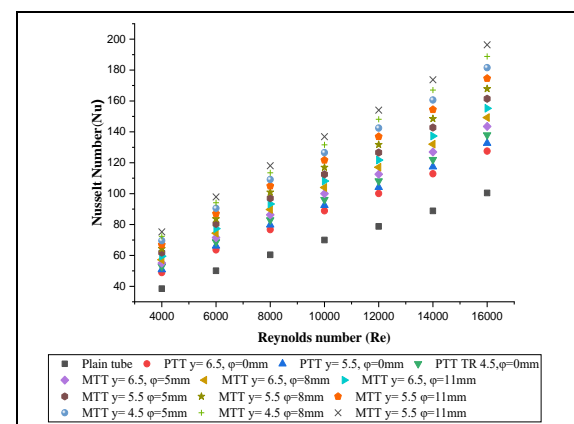


Figure 5. Plot of Nusselt number Vs Reynolds number for different diameter of semi-circular cut and twist ratio

In Figure 6. it can be seen that at lower Reynolds number the friction factor is higher. The lower twist creates extra hindrance in the path of the flow and hence there is higher friction factor. The maximum value of the friction factor has been observed to be 0.05005 over the range of study.

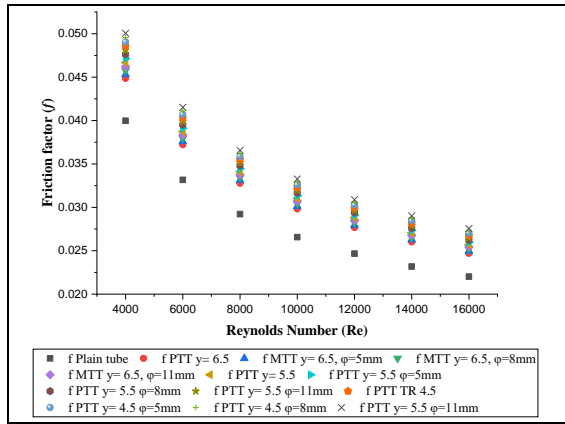


Figure 6. Plot of friction factor Vs Reynolds number for different diameter of semi-circular cut and twist ratio

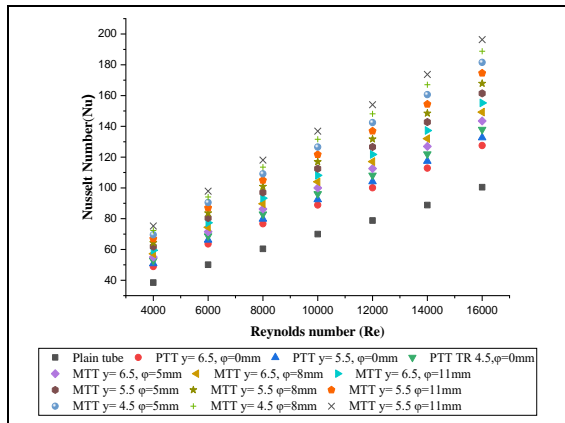


Figure 7. Plot of TPF Vs Reynolds number for different diameter of semi-circular cut and twist ratio

### 4.3 Velocity, Temperature and Turbulent Kinetic Energy(TKE) distribution at Re= 6000,

To examine the fluid dynamics and heat transfer attributes of a tubular heat exchanger featuring semi-circular cut twisted tapes (SCTT), it is valuable to utilize velocity contours, temperature contours, and contours depicting turbulent kinetic energy (TKE). In Figure 8(a), we can observe the radial velocity distribution within a tube at a distance of 500mm from the inlet. We have cases: a plain tube, a tube with SCTT at different cut sizes - ( $x=11\text{mm}, y=4.5$ ), ( $x=8\text{mm}, y=4.5$ ), and ( $x=5\text{mm}, y=4.5$ ). Analyzing the velocity contours reveals an interesting trend. Decreasing the cut size of the SCTT tapes leads to an increase in flow velocity along the tube wall and the face of the inserts. When compared to the velocity distribution in a plain tube, it's apparent that smaller SCTT cut sizes result in higher fluid velocity at the wall.

Conversely, larger cut sizes generate larger vortices. Furthermore, as the twist ratio of the tape diminishes, there's a noticeable rise in the intensity of the swirl motion. The SCTT tape introduces vortices that are uniformly spread across the tube. These vortices promote vigorous mixing of the fluid within the tube, compelling it to shift between the tube wall and the core.

Consequently, the presence of SCTT significantly shapes the flow pattern inside the tube, consequently impacting the temperature distribution as well.

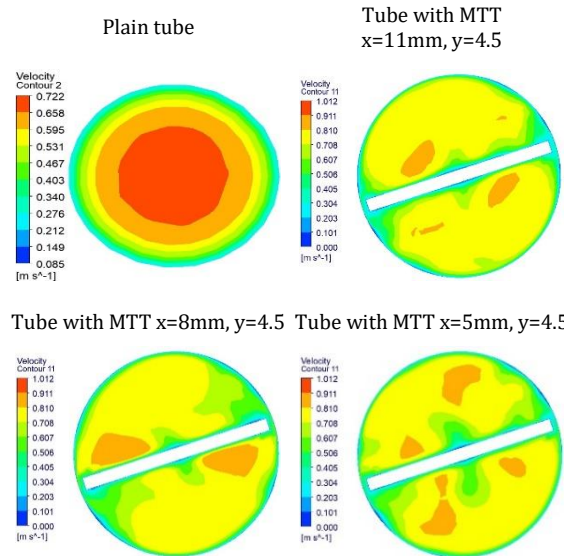


Figure 8(a) Radial velocity distribution inside the tube at L=500mm

Figure 8(b) depicting the radial temperature distribution at a plane situated 500mm from the inlet. In the case of the plain tube, a noticeable disparity emerges between temperatures near the hot wall and those at the centre. The thermal boundary layer adjacent to the wall remains undisturbed, while the fluid's temperature experiences minimal variation within the central zone. When examining larger cut sizes, distinctive temperature profiles become apparent from the contours. These contours unveil discernible zones of elevated temperature. As cut size increases, the extent of fluid mixing becomes more pronounced, leading to the dispersion of higher temperature zones across the tube.

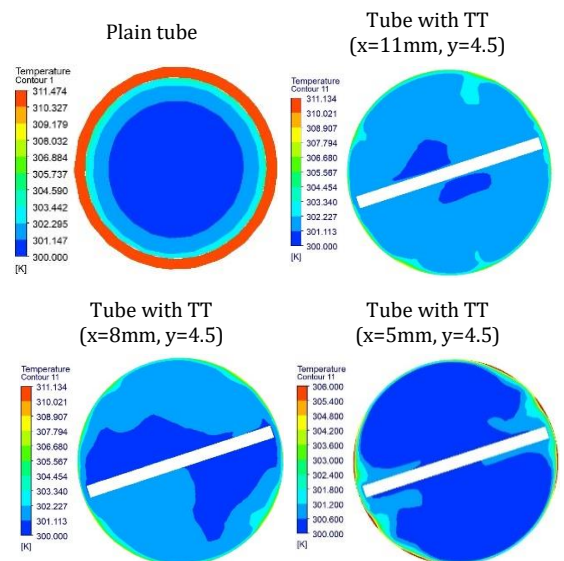
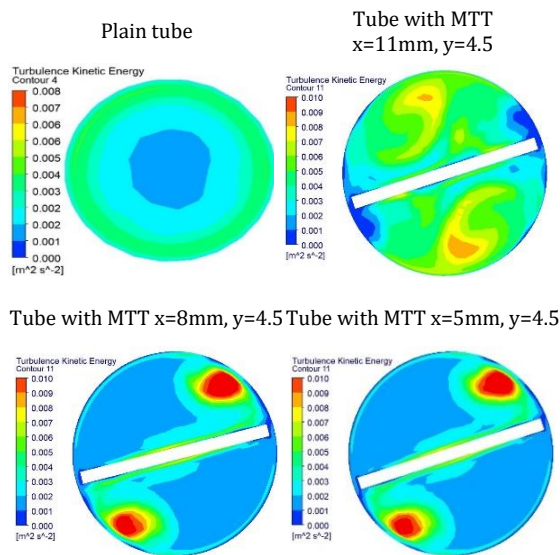


Figure 8(b) Radial Temperature distribution inside the tube at L=500mm

Figure 8(c), illustrating the distribution of radial turbulence kinetic energy (TKE) within the plane mentioned earlier and at the specified cut size. These TKE contours serve as a valuable tool for assessing fluid flow characteristics across different configurations of inserts, twist ratios, and insert cut sizes. The magnitude of vortex intensity engendered by SCTT tapes, contributing significantly to the augmentation of fluid intermixing and heat transfer, particularly as increment in cut size come into play.



**Figure 8(c)** Radial Turbulent Kinetic Energy distribution inside the tube at L=500mm

Comparative to the plain tube and traditional TT, the Turbulent Kinetic Energy (TKE) attains greater levels in instances featuring SCTT tapes. This amplification in TKE becomes even more pronounced as the twist ratio of the SCTT tapes undergoes reduction. It's discernible that the peak of TKE is attained when SCTT is employed at a twist ratio denoted by  $y=4.5$  and cut size  $x=11\text{mm}$ . This leads to the inference that a markedly twisted SCTT configuration would yield the most efficient heat transfer, especially when the twist ratio is taken into account.

They vividly capture the intensity of vortices generated by SCTT tapes, contributing to enhanced fluid intermixing and heat transfer by altering geometric parameters. Notably, the results show that the TKE is more pronounced in cases where SCTT tapes with a lower twist ratio ( $y=4.5$ ) and a larger cut ( $x=11\text{mm}$ ) are used compared to both plain tubes and twisted tapes without inserts.

#### 4.4 Thermal performance factor (TPF) analysis

The heat exchange quantification can be done by analysing the TPF. Fig.7. represents the variation in the TPF with Reynolds number. TPF for SCTT of different diameter and twist ratios analysed in the present study shows that it contributes to the energy saving in heat

transport methods. All through the study TPF found for SCTT is in the range of 1.141 to 1.801.

### Conclusions

In the present study, nine samples of the semi-circular-cut twisted tape inserts were examined. Experimental findings by Chaitanya Vashistha et al. [39] were used to verify the correctness of the numerical results. Important conclusions include the following:

- SCTT produce swirl near the wall of the tube which eat up the boundary layer. Also, this results in more fluid amalgamation, which significantly increases the rate of heat transmission.
- It has been discovered that employing SCTT leads to the wrecked boundary layer, fostering elevated heat transfer within the fluid medium. This outcome can be elucidated through the subsequent rationale: the periodic disturbances due to semi-circular cut induces a sudden redirection of fluid streamlines, thereby enhancing the confluence of fluids and elevating the mean fluid temperature.
- Moreover, the extremities and apices of the contorted wings, which prompt adjustments in the swirling direction, act akin to flow disturbers, cleaving fluid streams into distinct currents. These currents subsequently reunite after traversing these flow segregators, culminating in a potent collision between the flow streams.
- The twisted tapes without semi-circular cut have lower impact on the TPF. With SCTT the greatest value being 1.801. The present study demonstrating the industrial applicability of the tubular heat exchanger with SCTT.
- By introducing the SCTT a rise of 8.5%, 14.9%, and 19.1% in the Nu at twist ratios of 6.5, 5.5, and 4.5, correspondingly.
- The maximum increment in the friction factor is 243.2% with the cut size 11mm and twist ratio 4.5 at the lowest Reynolds number as compared to the plain tube.
- Since pressure drop is less severe than the increase in heat transmission, it may be concluded that the SCTT is a beneficial insert. Additional investigation is needed, and the SCTT's outside border has to be modified.

### Nomenclature

|    |   |
|----|---|
| A  | Cross sectional flow area                                 |
| As | Outer surface area of the heat exchanger, mm <sup>2</sup> |
| b  | Width of twisted tape, mm                                 |
| cp | Specific-heat capacity at constant pressure               |
| d  | Hydraulic diameter of the inner pipe, m                   |

|    |  |
|----|--|
| h  | Convective heat transfer coefficient, W/m <sup>2</sup> K |
| k  | Thermal conductivity W/mK                                |
| L  | Length of tube, mm                                       |
| m  | Mass flow rate of the fluid, kg/s                        |
| p  | Pitch ratio  |
| Nu | Nusselt number   |
| ΔP | Pressure drop  |
| Th | Hot fluid inlet temperature, °C                          |
| Tc | Cold fluid inlet temperature, °C                         |
| Q  | Rate of heat transfer, Watt                              |
| r  | Radius of pipe, mm                                       |
| x  | Cut diameter   |
| y  | Twist ratio  |
| Nu | Nusselt number   |
| ff | Friction factor  |

#### Greek Symbols

|   |                                       |
|---|---------------------------------------|
| μ | Dynamic viscosity, N-s/m <sup>2</sup> |
| η | TPF                                   |
| ρ | Density                               |
| φ | Diameter of semi-circular cut         |

#### Abbreviations

|        |  |
|--------|--|
| SCTT   | Semi-circular cut twisted tape                     |
| FVM    | Finite volume method                               |
| SIMPLE | Semi-implicit method for pressure-linked equations |
| DPHE   | Double pipe heat exchangers                        |
| HTR    | Heat transfer rate                                 |
| TT     | Twisted tape                                       |
| WC     | W-cut  |
| SC     | Square cut   |
| AA     | Alternate axis                                     |
| UC     | U-cut  |
| RC     | Rectangular cut                                    |
| CP     | Circular perforations                              |
| TC     | Triangular cut                                     |

## Acknowledgements

The author responsible for correspondence expresses gratitude for the fellowship assistance provided by the Ministry of Education (MoE), which is a part of the Government of India.

## Conflicts of Interest

The author declares that there is no conflict of interest regarding the publication of this manuscript. In addition, the authors have entirely observed the ethical issues, including plagiarism, informed consent, misconduct, data fabrication and/or falsification, double publication and/or submission, and redundancy.

## References

- [1] Wijayanta, A.T., Yaningsih, I., Aziz, M., Miyazaki, T. and Koyama, S., 2018. Double-sided delta-wing tape inserts to enhance convective heat transfer and fluid flow characteristics of a double-pipe heat exchanger. *Applied Thermal Engineering*, 145, pp.27-37. doi: 10.1016/j.applthermaleng.2018.09.009.
- [2] Abbasian Arani, A.A., Arefmanesh, A., and Uosofvand, H., 2017. Effect of baffle orientation on shell-and-tube heat exchanger performance. *Journal of Heat and Mass Transfer Research*, vol. 4, pp. 83–90, doi: 10.22075/jhmtr.2017.1577.1104
- [3] Wijayanta, A.T., Mirmanto and Aziz, M., 2020. Heat transfer augmentation of internal flow using twisted tape insert in turbulent flow. *Heat transfer engineering*, 41(14), pp.1288-1300.
- [4] Wijayanta, A.T., Yaningsih, I., Juwana, W.E., Aziz, M. and Miyazaki, T., 2020. Effect of wing-pitch ratio of double-sided delta-wing tape insert on the improvement of convective heat transfer. *International Journal of Thermal Sciences*, 151, p.106261.
- [5] Murali, G., Nagendra, B. and Jaya, J., 2020. CFD analysis on heat transfer and pressure drop characteristics of turbulent flow in a tube fitted with trapezoidal-cut twisted tape insert using Fe3O4 nano fluid. *Materials Today: Proceedings*, 21, pp.313-319.doi: 10.1016/j.matpr.2019.05.451.
- [6] Prasad, P.D., Gupta, A.V.S.S.K.S. and Deepak, K., 2015. Investigation of trapezoidal-cut twisted tape insert in a double pipe u-tube heat exchanger using Al2O3/water nanofluid. *Procedia Materials Science*, 10, pp.50-63. doi: 10.1016/j.mspro.2015.06.025.
- [7] Yaningsih, I., Wijayanta, A.T., Miyazaki, T. and Koyama, S., 2018, February. V-cut twisted tape insert effect on heat transfer enhancement of single phase turbulent flow heat exchanger. In *AIP Conference Proceedings (Vol. 1931, No. 1)*. AIP Publishing. doi: 10.1063/1.5024097.
- [8] Sanjay Kumar Singh & Arvind Kumar, "Experimental Study of Heat Transfer Enhancement from Dimpled Twisted Tape in Double Pipe Heat Exchanger," *Int. J. Mech. Prod. Eng. Res. Dev.*, vol. 10, no. 1, pp. 469–482, 2020, [Online]. Available: [http://www.tjprc.org/view-archives.php?page=132&keyword=&from\\_date=&to\\_date=&id=67&jtype=2&journal=67](http://www.tjprc.org/view-archives.php?page=132&keyword=&from_date=&to_date=&id=67&jtype=2&journal=67)
- [9] Diwaker, M.K. and Kumar, A., 2023. Impact of cut diameter on thermohydraulic performance of DPHE: an experimental analysis using internet of things (IoT) approach. *Heat and Mass Transfer*, pp.1-12. doi: 10.1007/s00231-023-03418-z.
- [10] Diwaker, M.K. and Kumar, A., 2023. Thermohydraulic performance of DPHE affected by triangular and semi-circular cut size on insert: IoT-based experimentation. *Case Studies in Thermal Engineering*, 43, p.102796. doi: 10.1016/j.csite.2023.102796.
- [11] Rezaei, A. and Baniamerian, Z., 2021. Hydro-thermal performance evaluation of nanofluids flow in double pipe heat exchanger: Effects of inner pipe cross section, circular or cam-shaped. *Journal of Heat and Mass Transfer Research*, 8(2), pp.283-299. doi: 10.22075/JHMTR.2021.22159.1327.
- [12] Yaningsih, I. and Wijayanta, A.T., 2017. Influences

- of pitch-length louvered strip insert on thermal characteristic in concentric pipe heat exchanger. In MATEC Web of Conferences, Vol. 101, p. 03014). EDP Sciences. doi: 10.1051/mateconf/201710103014.
- [13] Akbarzadeh, M., Rashidi, S., Keshmiri, A. and Shokri, N., 2020. The optimum position of porous insert for a double-pipe heat exchanger based on entropy generation and thermal analysis. *Journal of Thermal Analysis and Calorimetry*, 139, pp.411-426. doi: 10.1007/s10973-019-08362-x.
- [14] Soltani, M.M., Gorji-Bandpy, M., Vaisi, A. and Moosavi, R., 2022. Heat transfer augmentation in a double-pipe heat exchanger with dimpled twisted tape inserts: an experimental study. *Heat and Mass Transfer*, 58(9), pp.1591-1606. doi: 10.1007/s00231-022-03189-z.
- [15] Dandoutiya, B.K. and Kumar, A., 2021. CFD analysis for the performance improvement of a double pipe heat exchanger with twisted tape having triangular cut. *Energy Sources, Part A: Recovery, Utilization, and Environmental Effects*, pp.1-19. doi: 10.1080/15567036.2021.1946215.
- [16] Wijayanta, A.T., Kristiawan, B., Pranowo, Premono, A. and Aziz, M., 2019. Computational Fluid Dynamics Analysis of an Enhanced Tube with Backward Louvered Strip Insert. *Energies*, 12(17), p.3370.
- [17] Wijayanta, A.T., Pranowo, Mirmanto, Kristiawan, B. and Aziz, M., 2019. Internal flow in an enhanced tube having square-cut twisted tape insert. *Energies*, 12(2), p.306.
- [18] Arasteh, H., Salimpour, M.R. and Tavakoli, M.R., 2019. Optimal distribution of metal foam inserts in a double-pipe heat exchanger. *International Journal of Numerical Methods for Heat & Fluid Flow*, 29(4), pp.1322-3142.
- [19] Azmi, W.H., Sharma, K.V., Mamat, R. and Anuar, S., 2014. Turbulent forced convection heat transfer of nanofluids with twisted tape insert in a plain tube. *Energy procedia*, 52, pp.296-307.
- [20] Eiamsa-Ard, S., Ruengpayungsak, K., Thianpong, C., Pimsarn, M. and Chuwattanakul, V., 2019. Parametric study on thermal enhancement and flow characteristics in a heat exchanger tube installed with protruded baffle bundles. *International Journal of Thermal Sciences*, 145, p.106016. doi: 10.1016/j.ijthermalsci.2019.106016.
- [21] Esmaeilzadeh, A., Amanifard, N. and Deylami, H.M., 2017. Comparison of simple and curved trapezoidal longitudinal vortex generators for optimum flow characteristics and heat transfer augmentation in a heat exchanger. *Applied Thermal Engineering*, 125, pp.1414-1425. doi: 10.1016/j.applthermaleng.2017.07.115.
- [22] Saravanan, A. and Jaisankar, S., 2019. Heat transfer augmentation techniques in forced flow V-trough solar collector equipped with V-cut and square cut twisted tape. *International Journal of Thermal Sciences*, 140, pp.59-70. doi: 10.1016/j.ijthermalsci.2019.02.030.
- [23] Han, H., Li, B. and Shao, W., 2014. Multi-objective optimization of outward convex corrugated tubes using response surface methodology. *Applied thermal engineering*, 70(1), pp.250-262. doi: 10.1016/j.applthermaleng.2014.05.016.
- [24] García, A., Solano, J.P., Vicente, P.G. and Viedma, A., 2012. The influence of artificial roughness shape on heat transfer enhancement: Corrugated tubes, dimpled tubes and wire coils. *Applied Thermal Engineering*, 35, pp.196-201. doi: 10.1016/j.applthermaleng.2011.10.030.
- [25] Moya-Rico, J.D., Molina, A.E., Belmonte, J.F., Tendero, J.C. and Almendros-Ibáñez, J.A., 2020. Experimental characterization of a double tube heat exchanger with inserted twisted tape elements. *Applied Thermal Engineering*, 174, p.115234. doi: 10.1016/j.applthermaleng.2020.115234.
- [26] Bhuiya, M.M.K., Roshid, M.M., Talukder, M.M.M., Rasul, M.G. and Das, P., 2020. Influence of perforated triple twisted tape on thermal performance characteristics of a tube heat exchanger. *Applied Thermal Engineering*, 167, p.114769. doi: 10.1016/j.applthermaleng.2019.114769.
- [27] Nakhchi, M.E. and Esfahani, J.A., 2019. Numerical investigation of rectangular-cut twisted tape insert on performance improvement of heat exchangers. *International Journal of Thermal Sciences*, 138, pp.75-83. doi: 10.1016/j.ijthermalsci.2018.12.039.
- [28] Salem, M.R., Eltoukhey, M.B., Ali, R.K. and Elshazly, K.M., 2018. Experimental investigation on the hydrothermal performance of a double-pipe heat exchanger using helical tape insert. *International Journal of Thermal Sciences*, 124, pp.496-507. doi: 10.1016/j.ijthermalsci.2017.10.040.
- [29] Patel, B.V., Sarviya, R.M. and Rajput, S.P.S., 2022. Numerical investigations for the performance improvement of a tubular heat exchanger with anti-clockwise clockwise twisted tape inserts. *Energy Sources, Part A: Recovery, Utilization, and Environmental Effects*, 44(2), pp.4381-4397. doi: 10.1080/15567036.2022.2075993.
- [30] Yadav, V., Baghel, K., Kumar, R. and Kadam, S.T., 2016. Numerical investigation of heat transfer in extended surface microchannels. *International Journal of Heat and Mass Transfer*, 93, pp.612-622. doi: 10.1016/j.ijheatmasstransfer.2015.10.023.
- [31] Muñoz-Esparza, D. and Sanmiguel-Rojas, E., 2011. Numerical simulations of the laminar flow in pipes with wire coil inserts. *Computers & Fluids*, 44(1), pp.169-177. doi: 10.1016/j.compfluid.2010.12.034.
- [32] Karakaya, H. and Durmuş, A., 2013. Heat transfer and exergy loss in conical spring turbulators. *International Journal of Heat and Mass Transfer*, 60, pp.756-762. doi: 10.1016/j.ijheatmasstransfer.2013.01.054.

- [33] Nakhchi, M.E., Hatami, M. and Rahmati, M., 2020. Experimental investigation of heat transfer enhancement of a heat exchanger tube equipped with double-cut twisted tapes. *Applied Thermal Engineering*, 180, p.115863. doi: 10.1016/j.applthermaleng.2020.115863.
- [34] Sheikholeslami, M., Ganji, D.D. and Gorji-Bandpy, M., 2016. Experimental and numerical analysis for effects of using conical ring on turbulent flow and heat transfer in a double pipe air to water heat exchanger. *Applied Thermal Engineering*, 100, pp.805-819. doi: 10.1016/j.applthermaleng.2016.02.075.
- [35] Sheikholeslami, M. and Ganji, D.D., 2016. Heat transfer improvement in a double pipe heat exchanger by means of perforated turbulators. *Energy Conversion and management*, 127, pp.112-123.
- [36] Salem, M.R., 2020. Experimental investigation on the hydrothermal attributes of MWCNT/water nanofluid in the shell-side of shell and semi-circular tubes heat exchanger. *Applied Thermal Engineering*, 176, p.115438.
- [37] Eiamsa-Ard, S. and Seemawute, P., 2012. Decaying swirl flow in round tubes with short-length twisted tapes. *International Communications in Heat and Mass Transfer*, 39(5), pp.649-656.
- [38] Maddah, H., Aghayari, R., Mirzaee, M., Ahmadi, M.H., Sadeghzadeh, M. and Chamkha, A.J., 2018. Factorial experimental design for the thermal performance of a double pipe heat exchanger using Al<sub>2</sub>O<sub>3</sub>-TiO<sub>2</sub> hybrid nanofluid. *International Communications in Heat and Mass Transfer*, 97, pp.92-102. doi: 10.1016/j.icheatmasstransfer.2018.07.002.
- [39] Oni, T.O. and Paul, M.C., 2016. Numerical investigation of heat transfer and fluid flow of water through a circular tube induced with divers' tape inserts. *Applied Thermal Engineering*, 98, pp.157-168. doi: 10.1016/j.applthermaleng.2015.12.039.
- [40] Vashistha, C., Patil, A.K. and Kumar, M., 2016. Experimental investigation of heat transfer and pressure drop in a circular tube with multiple inserts. *Applied Thermal Engineering*, 96, pp.117-129. doi: 10.1016/j.applthermaleng.2015.11.077.
- [41] Guo, J., Fan, A., Zhang, X. and Liu, W., 2011. A numerical study on heat transfer and friction factor characteristics of laminar flow in a circular tube fitted with center-cleared twisted tape. *International Journal of Thermal Sciences*, 50(7), pp.1263-1270. doi: 10.1016/j.ijthermalsci.2011.02.010.
- [42] Ponnada, S., Subrahmanyam, T. and Naidu, S.V., 2019. A comparative study on the thermal performance of water in a circular tube with twisted tapes, perforated twisted tapes and perforated twisted tapes with alternate axis. *International Journal of Thermal Sciences*, 136, pp.530-538. doi: 10.1016/j.ijthermalsci.2018.11.008.
- [43] Noorbakhsh, M., Ajarostaghi, S.S.M., Zaboli, M. and Kiani, B., 2022. Thermal analysis of nanofluids flow in a double pipe heat exchanger with twisted tapes insert in both sides. *Journal of Thermal Analysis and Calorimetry*, 147(5), pp.3965-3977.
- [44] Chu, W.X., Tsai, C.A., Lee, B.H., Cheng, K.Y. and Wang, C.C., 2020. Experimental investigation on heat transfer enhancement with twisted tape having various V-cut configurations. *Applied Thermal Engineering*, 172, p.115148. doi: 10.1016/j.applthermaleng.2020.115148.
- [45] Murugesan, P., Mayilsamy, K. and Suresh, S., 2010. Heat transfer and friction factor studies in a circular tube fitted with twisted tape consisting of wire-nails. *Chinese Journal of Chemical Engineering*, 18(6), pp.1038-1042. doi: 10.1016/S1004-9541(09)60166-X.
- [46] Maddah, H., Aghayari, R., Farokhi, M., Jahanizadeh, S. and Ashtary, K., 2014. Effect of twisted-tape turbulators and nanofluid on heat transfer in a double pipe heat exchanger. *Journal of Engineering*, 2014. doi: 10.1155/2014/920970.
- [47] Patel, B.V., Sarviya, R.M. and Rajput, S.P.S., 2022. Numerical investigations for the performance improvement of a tubular heat exchanger with anti-clockwise clockwise twisted tape inserts. *Energy Sources, Part A: Recovery, Utilization, and Environmental Effects*, 44(2), pp.4381-4397.
- [48] Dandoutiya, B.K. and Kumar, A., 2022. W-cut twisted tape's effect on the thermal performance of a double pipe heat exchanger: a numerical study. *Case Studies in Thermal Engineering*, 34, p.102031.
- [49] Nakhchi, M.E. and Rahmati, M.T., 2021. Entropy generation of turbulent Cu-water nanofluid flows inside thermal systems equipped with transverse-cut twisted turbulators. *Journal of Thermal Analysis and Calorimetry*, 143(3), pp.2475-2484. doi: 10.1007/s10973-020-09960-w.
- [50] Murugesan, P., Mayilsamy, K., Suresh, S. and Srinivasan, P.S.S., 2011. Heat transfer and pressure drop characteristics in a circular tube fitted with and without V-cut twisted tape insert, *Int. Commun. Heat Mass Transf.*, vol. 38, no. 1, pp. 329-334, doi: 10.1016/j.icheatmasstransfer.2010.11.010.
- [51] Bhuiya, M.M.K., Chowdhury, M.S.U., Saha, M. and Islam, M.T., 2013. Heat transfer and friction factor characteristics in turbulent flow through a tube fitted with perforated twisted tape inserts. *International Communications in Heat and Mass Transfer*, 46, pp.49-57. doi: 10.1016/j.icheatmasstransfer.2013.05.012.